CARDIAC

Andreas H. Mahnken
Georg Mühlenbruch
Ralf Koos
Marco Das
Saskia Pohl
Sven Stanzel
Rolf W. Günther
Joachim E. Wildberger

Influence of a small field-of-view size on the detection of coronary artery calcifications with MSCT: in vitro and in vivo study

A. H. Mahnken (✉) ·
G. Mühlenbruch · M. Das · S. Pohl ·
R. W. Günther · J. E. Wildberger
Department of Diagnostic Radiology,
Aachen University of Technology,
Pauwelsstrasse 30,
52074 Aachen, Germany
e-mail: mahnken@rad.rwth-aachen.de
Tel.: +49-241-8088332
Fax: +49-241-8082499

R. Koos
Medical Clinic I,
Aachen University of Technology,
Aachen, 52074, Germany

S. Stanzel
Institute of Medical Statistics,
Aachen University of Technology,
Aachen, 52074, Germany

Abstract The purpose of this study is to asses the impact of small field-of-view (FOV) sizes on the detection of coronary artery calcifications using multislice-spiral computed tomography (MSCT). First, a static chest phantom containing calcium inserts was scanned 10 times using a standardized scan protocol. Secondly, 50 patients (28 male, 63.6±10.6 years) underwent cardiac MSCT using the same protocol. Images were reconstructed with three different FOV sizes (180×180, 220×220, 380×380 mm^2). Coronary calcium scoring and risk stratification were performed for each image series. In the phantom study, the Agatston score calculated with a FOV size of 180×180 mm^2 was 657.80± 20.05. At a FOV of 220×220 mm^2 and 380×380 mm^2, the corresponding values were 657.04±21.36 and 655.04±

20.74, respectively. The corresponding values in the patient study were 541.65± 869.87, 541.91±872.57 and 536.61± 867.81. No statistically significant differences in the calcium score were found comparing different FOV sizes. Significantly more lesions (p=0.00149) were detected in the patient study. Comparing the different FOV sizes of 180×180 mm^2 and 220×220 mm^2 (380×380 mm^2), four (six) patients had to be assigned to different risk groups. The use of small FOV sizes resulted in an improved detection of coronary calcifications influencing the risk stratification for further cardiac events in MSCT coronary calcium scoring.

Keywords Coronary vessels · Coronary vessels, calcification · Computed tomography (CT) · Multidetector row

Introduction

Coronary calcifications are a constituent of arteriosclerosis. Therefore, quantification of coronary calcifications has become a widely accepted diagnostic tool for risk stratification in suspected coronary artery disease. Moreover, this technique is also used to monitor drug therapy [1, 2]. Electron beam computed tomography (EBCT) was established as a gold standard for the evaluation of coronary artery calcifications. In recent years, multislice-spiral computed tomography (MSCT) has become widely accepted for detection and quantification of coronary artery calcifications [3–5]. However, coronary calcium scoring suffers several limitations. One major drawback of this technique, especially using EBCT, is the limited reproduc-

ibility of the coronary calcium score [6]. To improve accuracy and reproducibility of coronary calcium scoring, researchers have evaluated the influence of different examination parameters and scoring algorithms regarding the coronary calcium score. Points of image reconstruction, tube current as well as slice thickness, reconstruction interval and settings of the evaluation software were among the examination parameters that were investigated [7–11].

It wasn't until recently that the effect of spatial resolution on the coronary calcium score was evaluated [12]. An in vivo study showed an inverse relation between the coronary calcium score and the field of view (FOV) and indicated a higher sensitivity using a smaller FOV [13]. However, the possible range of FOV sizes, especially with respect to small FOV sizes, was not investigated. There-

fore, the aim of this study is to asses the impact of a small FOV size on the detection of coronary artery calcifications and the risk stratification in coronary calcium scoring.

Materials and methods

In vitro examination

For the in-vitro study, a non-moving CT-phantom (QRM, Moehrendorf, Germany) was examined. The phantom consists of an anthropomorphic chest phantom with lungs and spine inserts surrounded by soft-tissue equivalent material and a calibration insert [9]. The calibration insert at the position of the heart is a 100-mm-diameter cylinder containing three series of calcified cylinders with equal diameters and heights of 1, 3, and 5 mm. The calcium hydroxyapatite (CaHA) of each series of cylinders equals 200, 400, and 800 mg/cm^3, respectively. Moreover, the calibration insert contains two homogeneous cylinders with water (0±3 HU) and bone (CaHA density of 200 mg/cm^3) equivalent materials.

The phantom was positioned on the scanner table (SOMATOM Sensation 16, Siemens, Forchheim, Germany) and an ECG-signal with 60 beats per minute (bpm) was simulated (Laerdal Cardiac Rhythm Simulator, Laerdal, Stavanger, Norway). The phantom was scanned ten times after manual repositioning prior to each scan. A standardized examination protocol with 12×0.75 mm collimation, 2.8 mm table feed per rotation and a tube rotation time of 0.42 s was applied. Tube voltage was 120 kV with an effective tube current-time product of 133 mAs$_{eff}$.

Images were reconstructed at 60% of the RR-interval with an effective slice thickness of 3 mm and a reconstruction increment of 2 mm using a 512^2 matrix as described elsewhere [8]. The FOV was varied, using three different sizes. Two small FOV sizes adapted to the heart size as they were found in the literature and a large FOV size, covering the entire chest were used. This resulted in image reconstruction at an FOV of 180×180 mm^2, 220×220 mm^2 and 380×380 mm^2. The temporal resolution was fixed at 210 ms.

In vivo examination

Fifty consecutive patients (28 males; 22 females; mean age 63.6±10.6 years; mean heart rate 71±11.1 (39–99) bpm), who were referred for evaluation of coronary artery calcifications due to the presence of cardiovascular risk factors underwent retrospectively ECG-gated MSCT. Written informed consent was obtained from all patients.

All examinations were performed during a single breathhold of 18.8±2.2-s duration with the same 16-slice CT scanner (SOMATOM Sensation 16, Siemens) as the in vitro examinations. A standardized examination protocol

identical to the in vitro study was applied. Scanning parameters were as follows: 120 kV tube voltage, 133 mAs$_{eff}$ effective tube current-time product, 12×0.75 mm collimation, 2.8 mm table feed per rotation, 0.42 s tube rotation time. Effective radiation dose according to ICRP 60 was calculated (WinDose 2.1, Scanditronix Wellhöfer, Schwarzenbruck, Germany).

Image reconstruction was performed at 60% of the RR interval with an effective slice thickness of 3 mm and a reconstruction increment of 2 mm. Corresponding to the in vitro examination, three axial image series with a heart-size-adapted FOV of 180×180 mm^2 and 220×220 mm^2 as well as a full-chest-size-adapted FOV of 380×380 mm^2, were reconstructed in every patient using a 512^2 matrix. Temporal resolution of the image reconstruction algorithm was 105–210 ms, depending on the patient's heart rate [14].

Image analysis

For quantification of coronary artery calcifications, image data was transferred to an external workstation (Leonardo, Siemens, Germany). For each image series, the number of lesions, the coronary calcium score according to Agatston [15], calcium mass [9] and calcium volume were calculated applying a threshold of 130 Hounsfield Units (HU).

In the phantom study, the coronary calcium score, calcium mass and calcium volume were calculated for each of the three series of calcified cylinders. Results of the repeated phantom measurements were averaged for further analysis.

All patients underwent risk stratification according to Rumberger et al. [16]. Based on the Agatston score for each of the three image series, all patients were assigned to different levels of risk stratification regarding risk of future cardiac events. Depending on the Agatston score, cardiovascular risk was rated as follows: Agatston score 0=very low risk, Agatston score 1–10=low risk, Agatston score 11–100=moderate risk, Agatston score 101–400=moderately high risk, Agatston score>400=high risk. Patients with an Agatston score between 0 and 1 were considered to be at low risk.

To assess image noise, regions of interest (ROI; area: 2 cm^2) were placed in the water isodense calibration insert (in vitro) or the midsection of the left ventricle (in vivo). Measurements were performed on four consecutive axial slices. Mean and standard deviation (SD) were determined for each ROI, with the SD of the attenuation measurements ascribed to image noise. Results of the four measurements were averaged.

Statistical analysis

Results are given as mean±SD. To find differences in the above-mentioned parameters (Agatston Score, Calcium

Mass, Calcium Score, number of lesions) between the three image series, repeated measures ANOVA was used for the in vitro as well as the in vivo study. In case of statistically significant differences between the three image series in the global F-test of the repeated measures ANOVA, paired post-hoc *t* tests were performed in order to evaluate differences between each pair of image series. All statistical tests were conducted on a pre-specified significance level of 5%. Thus a *p*-value of $p<0.05$ was considered statistically significant. As this is an explorative study, an alpha adjustment was not performed. All statistical analyses were performed using the SAS statistical analysis software package, version 8.2 (SAS Institute, Cary, NC, USA).

Results

In vitro

At a FOV of 180×180 mm², the mean Agatston score measured in the phantom study was 657.80±20.05 (630.3–688.9). At FOV sizes of 220×220 mm² and 380×380 mm², the corresponding values were 657.04±21.36 (618.6–681.2) and 655.04±20.74 (624.3–683.4), respectively. With a FOV size of 180×180 mm², the mean attenuation value measured in the water isodense calibration insert was 3.5±0.9 HU. Detailed results are given in Table 1. Repeated measures ANOVA did not reveal significant differences of the coronary calcium score between the different image series (Agatston score: $p=0.77$; calcium mass: $p=0.70$; calcium volume: $p=0.95$).

In vivo

MSCT examinations were successfully completed in all patients. The mean temporal resolution was 143±48 ms. The calculated effective radiation dose according to ICRP 60 was 2.17±0.78 mSv for male patients and 3.14±0.93 mSv for female patients.

For one patient, no calcifications were detected in any of the three image series. In 49 patients, calcifications were present in at least one of the image series. Among these patients, two subjects presented with a single calcified lesion that was only seen in the image series reconstructed with a FOV of 180×180 mm² (Fig. 1). The Agatston score of each of these lesions was below 2. Repeated measures ANOVA did not reveal statistically significant differences between the different FOV sizes (Fig. 2) for the Agatston score ($p=0.33$, global F-test), the calcium mass ($p=0.29$, global F-test) and the calcium volume ($p=0.33$, global F-test), but did, however, for the number of lesions ($p=0.0149$, global F-test). Post-hoc *t* tests using a FOV size of 180×180 mm² when compared to 380×380 mm² ($p=0.0015$) showed a significant increase in the number of lesions, while the difference was not statistically significant comparing FOV

Table 1 Coronary calcifications as quantified from phantom measurements

	Lesion series	FOV [mm²]		
		180×180	220×220	380×380
Volume score [mm³]	Total	645.21±16.13 (617.9–665.5)	645.82±16.20 (617.9–664.9)	645.33±17.36 (617.3–665.4)
Calcium mass [mg]		164.55±6.82 (155.37–173.05)	164.65±6.77 (155.28–172.14)	163.64±6.65 (156.24–173.50)
Agatston score		657.80±20.05 (630.30–688.9)	657.04±21.36 (618.60–681.20)	655.04±20.74 (624.30–683.40)
Volume score [mm³]	200 mg CaHA/cm³	121.25±5.75 (112.60–130.70)	121.66±5.35 (114.50–130.90)	122.11±5.84 (113.80–131.60)
Calcium mass [mg]		17.46±1.31 (15.31–19.08)	17.58±1.24 (15.64–19.25)	17.64±1.44 (15.47;19.47)
Agatston score		76.58±8.65 (67.20–87.10)	76.02±7.79 (67.90–88.50)	73.50±9.53 (62.80–90.10)
Volume score [mm³]	400 mg CaHA/cm³	212.41±5.41 (201.9–218.90)	211.56±5.91 (200.60±219.20)	211.36±7.41 (202.60–222.60)
Calcium mass [mg]		43.81±1.63 (41.37–45.78)	43.72±1.66 (41.02–45.86)	43.49±1.85 (40.95–46.11)
Agatston score		219.34±10.33 (205.40–232.80)	219.44±9.53 (202.90–231.90)	217.30±10.41 (205.50–235.80)
Volume score [mm³]	800 mg CaHA/cm³	312.31±13.17 (283.60±323.30)	312.60±13.53 (283.20±323.90)	311.86±14.30 (282.90±325.20)
Calcium mass [mg]		103.27±6.14 (92.62±109.61)	103.35±6.15 (92.74±109.35)	102.51±6.07 (93.08–110.21)
Agatston score		361.14±15.97 (327.20±384.30)	361.57±16.13 (328.90±387.10)	364.25±17.88 (332.00±387.10)
Mean attenuation [HU]		3.5±0.9	3.6±0.6	3.4±0.7
Noise [HU]		0.8±0.3	0.9±0.3	0.8±0.4

Minimum and maximum values are provided in brackets

Fig. 1 Retrospectively ECG-gated MSCT for coronary artery calcium scoring. Image reconstruction with small FOV sizes shows an improved sensitivity for the detection of small calcifications. A calcified lesion of the right coronary artery (*arrow*) detected at a FOV of 180×180 mm^2 (**a**) does not reach the threshold of 130 HU applying FOV sizes of 220×220 mm^2 (**b**) or 380×380 mm^2 (**c**). Note that there is only a minor difference in the FOV size between image (a) and image (b), but a clinically relevant difference of the coronary calcium score
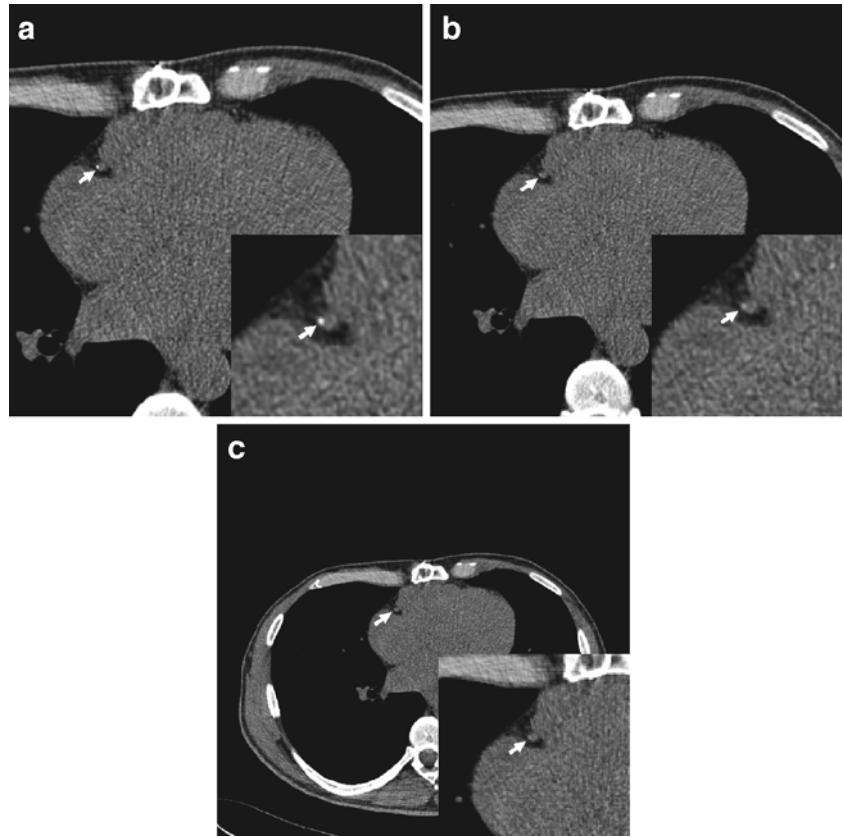
sizes of 180×180 mm^2 and 220×220 mm^2 (*p*=0.1501) or comparing FOV sizes of 220×220 mm^2 and 380×380 mm^2 (*p*=0.1848). Detailed results are summarized in Table 2.

In the comparison of FOV sizes of 180×180 mm^2 and 220×220 mm^2, four of the patients (8%) had to be assigned to different risk groups according to the risk stratification

by Rumberger et al. [16]. In the comparison of FOV sizes of 180×180 mm^2 and 380×380 mm^2, six patients (12%) had to be assigned to different risk groups, while two patients (4%) had to be transferred to a different risk group when comparing FOV sizes of 220×220 mm^2 and 380×380 mm^2 (Table 3).
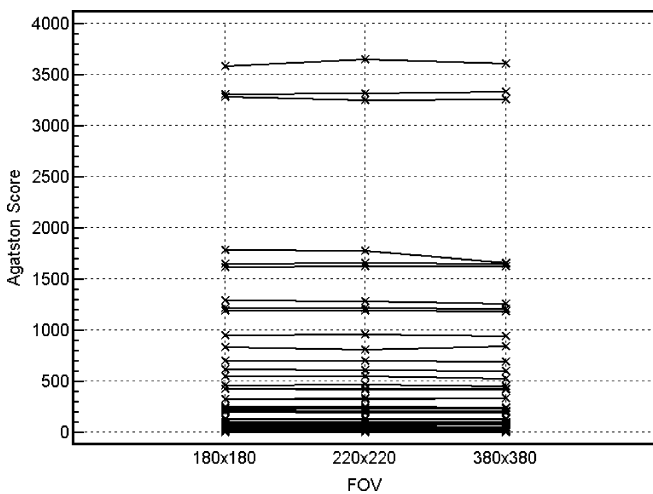
Fig. 2 The dot-and-line diagram shows a negligible effect of the FOV size on the total coronary calcium burden as measured with the Agatston score

Table 2 Coronary calcifications and image noise for the different FOV sizes

	FOV [mm^2]		
	180×180	220×220	380×380
Lesions [n]	11.20±9.17 (1–32)	10.78±8.76 (0–32)	10.42±8.98 (0–33)
Volume score [mm^3]	363.3±612.27 (0–2442.50)	362.80±611.23 (0–2443.20)	360.94±609.75 (0–2446.10)
Calcium mass [mg]	169.97±289.32 (0.06–1305.87)	169.10±287.87 (0–1274.47)	168.51±286.45 (0–1276.24)
Agatston score	541.65±869.87 (0.20–3585.70)	541.91±872.57 (0–3647.20)	536.61±867.81 (0–3608.40)
Mean attenuation [HU]	46.2±6.5	46.0±7.1	46.0±6.9
Noise [HU]	19.9±2.4	19.3±2.2	19.6±1.8

Minimum and maximum values are given in brackets

Table 3 Results of the risk stratification for future cardiac events according to Rumberger et al. [16]

Risk level	FOV (mm^2)		
	180×180	220×220	380×380
Very low (n)	1	3	4
Low (n)	7	6	6
Moderate (n)	15	14	13
Moderately high (n)	9	9	9
High (n)	18	18	18

The FOV size affects risk stratification in patients with very low to moderate risk of future cardiac events, whereas the FOV size does not affect the risk level in patients considered as moderately high or high risk (n=number of patients)

Discussion

Spatial resolution is known to influence the coronary calcium score in cardiac CT [12]. This effect is explained by the partial volume effect. A change in the FOV size and, as a consequence in the voxel size, affects the degree of partial volume averaging within voxels. As the detection of coronary calcifications is based on a fixed threshold, partial volume effect due to different voxel size will affect the detected lesion size and therefore the coronary calcium score. The Agatston score in particular can be expected to be prone to this type of artefact since it depends on a step function of a weighting factor [15]. In clinical routine, a wide range of examination protocols with varying spatial resolution are used for coronary calcium scoring. While most studies use a slice thickness of 3 mm (z-axis resolution), the FOV size varies from 180×180 mm^2 to 430×430 mm^2 [8, 17–21], resulting in a broad bandwidth of spatial resolution in the x/y-plane. Some studies even used different FOV sizes in the same patient group [20, 22]. This problem was first investigated in a patient study by Hong et al. [13], and showed a negligible effect of the FOV size on the total calcium score. Risk stratification nonetheless was affected by FOV size. However, this study group investigated the application of a limited range of relatively large FOV sizes and failed to show an influence of small heart-size-adapted FOV sizes on the risk stratification as well as on the coronary calcium score.

From our experience, even differences between small FOV sizes influence the detection of small calcifications and therefore the patients risk stratification. Thus, regarding the detection and quantification of coronary calcifications, we investigated the use of small FOV sizes in comparison to full chest-size-adapted FOV. The small FOV sizes were chosen to analyze the influence of minor changes in the voxel size in the x/y-plane regarding the detection of coronary artery calcifications. The single large FOV size was selected to investigate the complete range of FOV sizes on the calcium score while keeping the amount of data in acceptable ranges. A phantom study was performed prior to the patient study in order to limit parameters that potentially influence the coronary calcium score, especially motion artefacts.

The results of the phantom study did not show a statistically significant influence of the three investigated FOV sizes on the coronary calcium score. However, although a non-moving cardiac phantom was used, repeated phantom measurements with the same FOV presented variability in the coronary calcium score of approximately 9% (Table 1). The low-density insert (200 mg CaHA/cm^3) showed the highest variability in repeated measurements. Variation of repeated measurements exceeded the expected influence of the FOV size on the coronary calcium score. As a consequence, the lack of statistical significance was to be expected, leaving room for a potentially relevant influence of the FOV size on the individual patients coronary calcium score.

In the patient study, the coronary calcium score did not show significant differences when applying the same three different FOV sizes as in the phantom study. Risk stratification however was affected by varying FOV sizes. Estimated risk for further cardiac events changed in 8% of patients when comparing a FOV of 180×180 mm^2 and 220×220 mm^2 and in 12% of patients when comparing a FOV of 180×180 mm^2 and 380×380 mm^2. These differences only occurred in small lesions, however, small lesions are known to be of particular prognostic significance [23]. In two patients, some coronary calcifications were only detected by use of the smallest FOV size of 180×180 mm^2 (Fig. 1). Moreover, images with the smallest FOV size revealed significantly more calcified lesions than images reconstructed with the largest FOV size. Thus, the use of small FOV sizes results in an improved sensitivity for the detection of coronary calcifications. While these lesions do not substantially contribute to the total calcium burden, this finding is of interest in regards to risk stratification. Besides the total amount of calcium, the presence or absence of calcified lesions is known to be important. Improved sensitivity in the detection of coronary artery calcifications will be of special interest in patients with small calcifications, as the absence of coronary artery calcifications is considered a key indicator for the absence of obstructive coronary artery disease [24]. As a consequence, a standardized, small as possible heart-size-adapted FOV should be used for coronary calcium scoring. From our experience, all patients undergoing coronary calcium scoring for coronary risk assessment can be examined with a FOV of 180×180 mm^2. A larger FOV might only be needed in those patients with an enlarged heart due to several cardiac disorders. Moreover, the FOV has to be kept constant during follow-up to achieve the best interscan comparability.

There are some limitations to this study. First, only a limited number of patients were included in this study. Second, only three different FOV sizes were analysed.

Lastly, a rigid risk stratification system was used instead of an age and sex adjusted score [25]. Moreover, it has to be kept in mind that the risk stratification schema used in this study was established for EBCT, because there is a known difference between MSCT and EBCT for coronary calcium scoring [4]. Therefore, the actual risk of further cardiac events may differ from the estimated risk calculated from MSCT data. Nevertheless, in all risk stratification systems, the differentiation between coronary artery calcifications being present or not is considered to be of major importance.

In conclusion, the results of our study show a negligible effect of the FOV size on the coronary calcium score, whereas the number of lesions detected by CT differs. From our results, the use of the smallest possible FOV size can be recommended. A constant FOV size for each patient is needed to ensure data comparability particularly for follow-up examinations.

References

1. Hoffmann U, Derfler K, Haas M, Stadler A, Brady TJ, Kostner K (2003) Effects of combined low-density lipoprotein apheresis and aggressive statin therapy on coronary calcified plaque as measured by computed tomography. Am J Cardiol 91:461–464
2. Achenbach S, Ropers D, Pohle K, Leber A, Thilo C, Knez A, Menendez T, Maeffert R, Kusus M, Regenfus M, Bickel A, Haberl R, Steinbeck G, Moshage W, Daniel WG (2002) Influence of lipid-lowering therapy on the progression of coronary artery calcification: a prospective evaluation. Circulation 106:1077–1082
3. Carr JJ, Crouse JR, Goff DC, D'Agostino RB, Peterson NP, Burke GL (2000) Evaluation of subsecond gated helical CT for quantification of coronary artery calcium and comparison with electron-beam CT. Am J Roentgenol 174:915–921
4. Becker CR, Kleffel T, Crispin A, Knez A, Young J, Schoepf UJ, Haberl R, Reiser MF (2001) Coronary artery calcium measurement: agreement of multirow detector and electron beam CT. Am J Roentgenol 176:1295–1298
5. Knez A, Becker C, Becker A, Leber A, White C, Reiser M, Steinbeck G (2002) Determination of coronary calcium with multi-slice spiral computed tomography: a comparative study with electron-beam CT. Int J Cardiovasc Imaging 18:295–303
6. Thompson BH, Stanford W (2004) Imaging of coronary calcification by computed tomography. J Magn Reson Imaging 19:720–733
7. Hong C, Bae KT, Pilgram TK, Suh J, Bradley D (2002) Coronary artery calcium measurement with multi-detector row CT: in vitro assessment of effect of radiation dose. Radiology 225:901–906
8. Mahnken AH, Wildberger JE, Sinha AM, Flohr T, Truong HT, Krombach GA, Gunther RW (2002) Variation of the coronary calcium score depending on image reconstruction interval and scoring algorithm. Invest Radiol 37:496–502
9. Ulzheimer S, Kalender WA (2003) Assessment of calcium scoring performance in cardiac computed tomography. Eur Radiol 13:484–497
10. Mao S, Child J, Carson S, Liu SC, Oudiz RJ, Budoff MJ (2003) Sensitivity to detect small coronary artery calcium lesions with varying slice thickness using electron beam tomography. Invest Radiol 38:183–187
11. van Ooijen PM, Vliegenthart R, Witteman JC, Oudkerk M (2005) Influence of scoring parameter settings on Agatston and volume scores for coronary calcification. Eur Radiol 15:102–110
12. Kaufman L, Mineyev M, Carlson J, Goldhaber D, Rumberger J (2003) Coronary calcium scoring: modelling, predicting and correcting for the effect of CT scanner spatial resolution on Agatston and volume scores. Phys Med Biol 48:1423–1436
13. Hong C, Pilgram TK, Zhu F, Bae KT (2004) Coronary artery calcification: effect of size of field of view on multidetector row CT measurements. Radiology 233:281–285
14. Flohr T, Ohnesorge B (2001) Heart rate adaptive optimization of spatial and temporal resolution for electrocardiogram-gated multislice spiral CT of the heart. J Comput Assist Tomogr 25:907–923
15. Agatston AS, Janowitz W, Hildner FJ, Zusmer NR, Viamonte M, Detrano R (1990) Quantification of coronary artery calcium using ultrafast computed tomography. J Am Coll Cardiol 15:827–832
16. Rumberger JA, Brundage BH, Rader D, Kondos G (1999) Electron beam computed tomographic coronary calcium scanning: a review and guidelines for use in asymptomatic persons. Mayo Clin Proc 74:243–252
17. Leber AW, Knez A, Mukherjee R, White C, Huber A, Becker A, Becker CR, Reiser M, Haberl R, Steinbeck G (2001) Usefulness of calcium scoring using electron beam computed tomography and noninvasive coronary angiography in patients with suspected coronary artery disease. Am J Cardiol 88:219–223
18. Herzog C, Britten M, Balzer JO, Mack MG, Zangos S, Ackermann H, Schaechinger V, Schaller S, Flohr T, Vogl TJ (2004) Multidetector-row cardiac CT: diagnostic value of calcium scoring and CT coronary angiography in patients with symptomatic, but atypical, chest pain. Eur Radiol 14:169–177
19. Detrano R, Hsiai T, Wang S, Puentes G, Fallavollita J, Shields P, Stanford W, Wolfkiel C, Georgiou D, Budoff M, Reed J (1996) Prognostic value of coronary calcification and angiographic stenoses in patients undergoing coronary angiography. J Am Coll Cardiol 27:285–290

20. Takahashi N, Bae KT (2003) Quantification of coronary artery calcium with multi-detector row CT: assessing inter-scan variability with different tube currents—pilot study. Radiology 228:101–106

21. Shemesh J, Koren-Morag N, Apter S, Rozenman J, Kirwan BA, Itzchak Y, Motro M (2004) Accelerated progression of coronary calcification: four-year follow-up in patients with stable coronary artery disease. Radiology 233:201–209

22. Hong C, Pilgram TK, Zhu F, Bae KT (2004) Is coronary artery calcium mass related to Agatston score? Acad Radiol 11:286–292

23. Ehara S, Kobayashi Y, Yoshiyama M, Shimada K, Shimada Y, Fukuda D, Nakamura Y, Yamashita H, Yamagishi H, Takeuchi K, Naruko T, Haze K, Becker AE, Yoshikawa J, Ueda M (2004) Spotty calcification typifies the culprit plaque in patients with acute myocardial infarction: an intravascular ultrasound study. Circulation 110:3424–3429

24. Raggi P, Callister TQ, Cooil B, He ZX, Lippolis NJ, Russo DJ, Zelinger A, Mahmarian JJ (2000) Identification of patients at increased risk of first unheralded acute myocardial infarction by electron-beam computed tomography. Circulation 101:850–855

25. Hoff JA, Chomka EV, Krainik AJ, Daviglus M, Rich S, Kondos GT (2001) Age and gender distributions of coronary artery calcium detected by electron beam tomography in 35,246 adults. Am J Cardiol 87:1335–1339